No. 47 NUMERICAL CALCULATIONS ON A WIDE ANGLE FILTER LENS

by J. A. DEN BOER AND ALVAR P. WILSKA

June 9, 1964

ABSTRACT

Filter lenses with unconventionally shaped electrodes and with large image angles were recently designed in our laboratory. The ray trajectories of one of these lenses are computed as solutions of the general ray equation. The chromatic aberrations are determined, as well as the usable image angle. Other properties of the lens are briefly discussed.

1. Introduction

Boersch (1947) has pointed out that the contrast of electron-optical images can be improved by filtering the inelastically scattered electrons out of the beam. Electrostatic lenses in which the minimum of the axial potential is of the order of 10 V above the cathode potential have the desired filtering properties. It has been shown (Boersch, 1949, 1953; Beaufils, 1959; Catalina, 1959; Möllenstedt and Rang, 1951; Schiekel, 1952; Lippert, 1955; Hahn, 1959) that the aberrations of such filter lenses can be made small if certain precautions are taken. The image angles of the best of these lenses appear to be too small, however, to be useful for what we think is the best application of a filter lens, i.e., as a projector in an electron microscope.

In the preceding paper (Wilska and den Boer, 1964), designs for a number of filter lenses giving image angles of more than 30° were presented. In the present paper, the performance of one of these lenses is studied more extensively: the trajectories of the electrons are computed, and optical properties are derived from these computations.

2. Calculation Techniques

As the electrons in the filter lens are expected to make large angles with the axis, the trajectories cannot be found with the paraxial ray equation, but should be solutions of the general ray equation. Thus, the potential in the filter lens must be calculated for a sufficient number of representative points on an axial cross-section through the lens. The potentials at the lattice points of a square lattice imagined to be in this cross-section are obtained by relaxation. In this relaxation lattice, the electrodes are represented by rows of lattice points kept at the electrode potential. The potential at each lattice point is calculated from the potentials at four neighboring lattice points. The relaxation is carried out in four stages. In the first stage, the lattice is extended in the radial direction. In each following stage, the fineness of the lattice is increased and its radial extension reduced by a factor of two. The final potentials obtained in each stage are used as the initial potentials of the next stage.

The general ray equation is (Zworykin, *et al.*, 1954, page 401):

$$r'' = \frac{(1+r'^2)}{2V}\left[\frac{\partial V}{\partial r} - r'\,\frac{\partial V}{\partial z}\right] \qquad (1)$$

The integration of this equation is carried out step by step with a fifth order predictor-corrector method, analogous to similar methods described by Hammingh (1962) for first-order differential equations. In practice, the method is satisfactory as to stability. In the general ray equation, the terms V, $\partial V/\partial r$, and $\partial V/\partial z$ are replaced by fourth-order and third-order expressions in the potentials at the surrounding lattice points. The step length of the predictor-corrector method is chosen by the computer in such a way

that the error in each step remains small enough not to affect the final solution. The smallest possible step length, however, is equal to the unit of the relaxation lattice, so that, in most cases, the required accuracy is not attained in the strongest part of the lens, thus limiting the method.

3. *Properties of the Lens*

The shape of the electrodes of the investigated lens is shown in Figure 1. The important coordinate

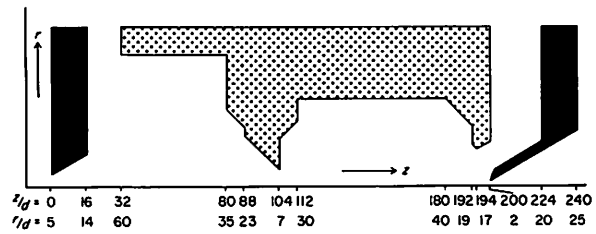

Fig. 1. Shape of the electrodes of the filter lens with coordinates along the r and z axes.

values are given along the r and z axes. The unit of length is the unit distance d of the relaxation lattice. In order to approach the experimental conditions for the lens, the exit pupil of the objective is located at $z = -1250\ d$, the image plane at $z = 800\ d$, and the accelerating voltage is 6500 V. The size of the lens model becomes equal to the size of the experimental lens if $d = 0.16$ mm.

In Figure 2, the potential distributions in the lens are given for four values of the potential V_c on the central electrode, by means of series of equipotentials. One distribution is computed, and subsequent distributions are derived from the first by changing the level of the zero potential. The difference in the potentials near the outer electrodes is negligible. For each value of V_c, Figure 2 shows two rays entering the lens, at $r_0 = d$ and $r_0 = 3d$. Figure 2 can also be regarded as showing the trajectories of electrons with different energy losses.

The magnification M of the lens at the image plane is calculated from the final slope of the rays and is plotted in Figure 3 as a function of V_c for different values of r_0. The intermediate image in the object space of the filter lens is assumed in this calculation to be located at $z = 0$. The maximal magnification is about 62x.

In order to minimize chromatic aberrations, the lens should be operated at this maximum of magnification. This requirement cannot be met completely. In particular, the finite energy variation ΔV of the transmitted electrons, and the dependence of the potential V_c, where the maximum of magnification is reached, upon the incident height r_0 must be considered (Bykhovskaya and Der-Shvarts, 1959). Ac-

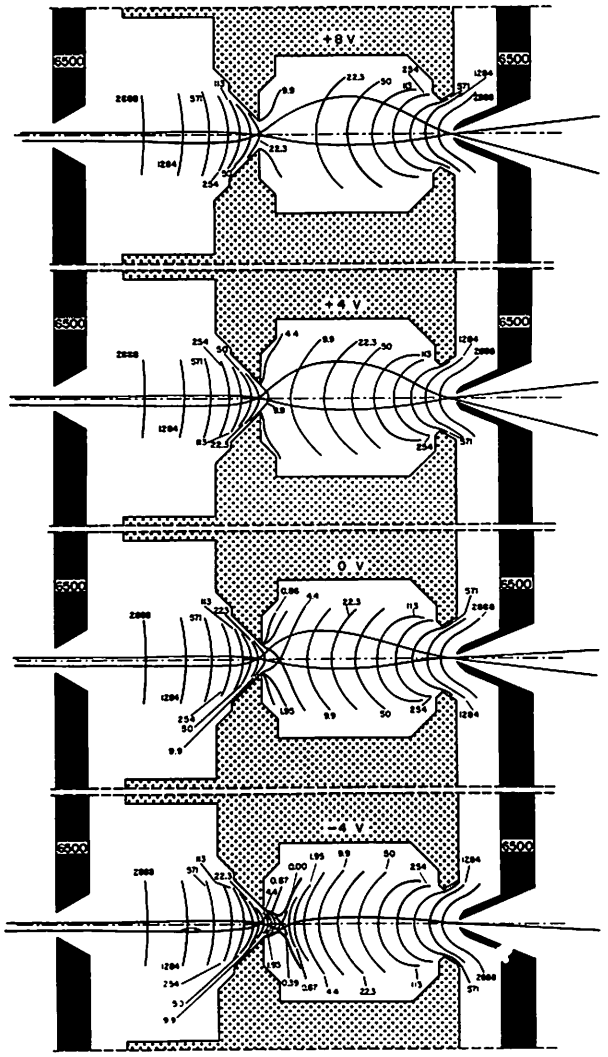

Fig. 2. Equipotentials and trajectories in the filter lens, calculated for four different values of the potential on the central electrode.

cordingly, δ_{cm}, the chromatic aberration referred to the plane of the intermediate image, can be written as:

$$\delta_{cm} = \frac{1}{M} r_0 \left[\frac{\partial M}{\partial V} \Delta V + \frac{\partial^2 M}{\partial V^2} \Delta V^2 + \frac{\partial^2 M}{\partial V_r^2} \Delta V r_0^2 \right]. \quad (2)$$

If no inelastically scattered electrons reach the image screen, it is safe to assume $\Delta V = 0.5V$. From Figure 3, the value of δ_{cm} can then be estimated. Such estimates are given in Table 1 for several values of V_c and r_0. Figure 3 shows that the distortion in

the lens is small. If stringent requirements are not set for the distortion of the image, and if the other geometric aberrations are small (Schiekel, 1952), then the field of view will be limited by the acceptable size of δ_{cm}. If the minimum resolution required at the image plane is 0.12 d, or 20 μ in the experiment, so as not to be excessive in view of the resolving power of the photographic plate, then the following requirement must be met:

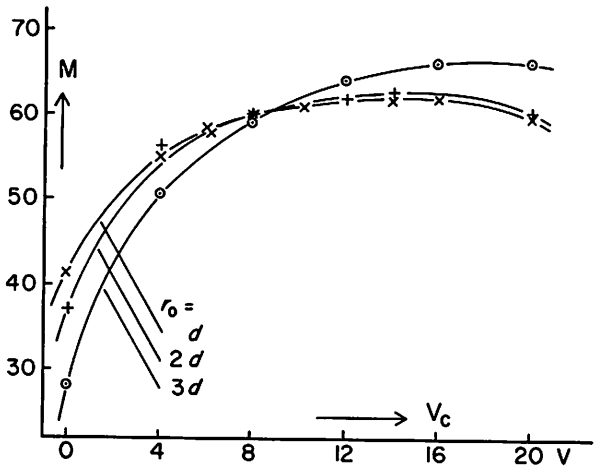

Fig. 3. Variation of the magnification M on the image screen with the potential of the central electrode V_c for three different parts of the lens, characterized with rays entering the lens at r_0 = 160, 320, and 480 μ (d = 0.16 mm).

$$\delta_{cm} < \frac{0.12\,d}{M} \sim 2 \cdot 10^{-3} d. \qquad (3)$$

Table 1 gives the allowed image angle α, estimated from Equation (3) and the values of δ_{cm} for different values of r_0. The number of lines in the image is proportional to the tangent of this angle α.

The resolution near the center of the image is limited by δ_{ca}, the chromatic aberration on the axis of the lens. The value of δ_{ca} depends mainly on the variation in the location of z_H of the first principal plane of the lens with changing V_c, and on the aperture γ of the pencils of rays in the object space of the lens.

TABLE 1

THE CHROMATIC ABERRATION* OF THE FILTER LENS δ_{cm}; AND THE ALLOWED IMAGE ANGLE α.**

V_c	$r_0 = d$	$r_0 = 2d$	$r_0 = 3d$	α
8	0.7	1.6	5.5	5°
10	0.4	1.0	3.9	10
12	0.2	0.6	2.7	16
14	0.04	0.3	1.8	25
16	0.1	0.2	0.6	34
18	0.5	0.5	0.4	40

*Derived from the computed magnifications in Fig. 3, if V = 0.5 V and d = 0.16 mm.
**Of the region of the image in which the resolution is better than 20 μ.

The following relation is easily derived:

$$\delta_{ca} = \gamma \frac{\partial z_H}{\partial V} \Delta V. \qquad (4)$$

In order to be able to calculate this aberration for various choices of V_c and r_0, a second set of rays is computed. Each of these rays enters the lens at the same height as a ray of the first set and remains close to this ray in the lens. Each pair of rays defines a value for z_H. These values are listed in Table 2.

TABLE 2

THE LOCATION z_H OF THE FIRST PRINCIPAL PLANE FOR DIFFERENT VALUES OF THE POTENTIAL OF THE CENTRAL ELECTRODE V_c AND THE INCIDENT HEIGHT r_0*

V_c	$r_0 = d$	$r_0 = 2d$	$r_0 = 3d$
4	348	110	83
8	216	127	91
12	133	142	132
20	98	192	221

*Maximal error = ± 15.

Although accuracy is limited by the large errors in z_H, it is estimated that at V_c = 16 V, $\partial z_H/\partial V = 5\,d$ (mm/V). With $\gamma = 10^{-4}$, Equation (4) then gives

$$\delta_{ca} = 0.2 \cdot 10^{-3} d. \qquad (5)$$

If we now compare Equation (5) with Figure 2, we see that the chromatic aberration on the axis does not limit the resolution of the lens. In the center of the image the resolution is better than required.

4. Discussion

At V_c = 16 V, the number of lines in the image is 3100 and the image angle is 34°. These properties make the lens suitable for use as a projector. The large image angle is due to the location of the exit pupil near the aperture of the third electrode. In the present lens this is achieved by giving the third electrode the shape of a cone, which brings its aperture close to the central electrode.

If the lens is operated at V_c = 16 V, the minimal potential on the axis is 20.4 V. The ratio between this potential and the accelerating potential is large compared with the same ratio for lenses described in the literature. Evidently, the large value of this ratio is related to the thick central electrode (Lippert, 1955).

In our experiment, the lens had slightly different properties. When the lens was operated at $V_c = 4$ V, the image angle was 38°, the central electrode potential was 10 V, and the magnification was 53x. The cause of these differences may be that the diameters of the electrode apertures in the computations were, in general, not quite equal to the corresponding diameters in the real lens, since only truncated values could be allowed, and because the rounding off of the edge of the aperture could not be taken into account. However, the model represents the actual lens quite well.

The images produced by this lens usually have a small luminous spot in the center. The spot disappears when there is no object and is bright when the object is thick, but still partially penetrable by the electrons. It is therefore assumed that the spot arises from those slowed down electrons for which the lens is telescopic (see Fig. 2d).

Acknowledgments. This work was supported by the National Aeronautics and Space Administration under Grant NsG-487 and by the Public Health Service under Grant GM 11852-01.

REFERENCES

Beaufils, R. 1959, *C. R. Acad. Sci., 248,* 3145–3147.

Boersch, H. 1947, *Z. Naturforsch, 2a,* 615–632.

———. 1949, *Optik,* 7, 436–450.

———. 1953, *Z. Phys., 134,* 156–164.

Bykhovskaya, L. N. and Der-Shvarts, G. V. 1959, *Radiotekhnika i elektronika, 4,* 1145–1152.

Catalina, F. 1959, *An. Real. Soc. Esp. Fis. Quim. Madrid, 55a,* 15–22.

Hahn, E. 1959, *Exper. Tech. Phys., 7,* 258.

Hammingh, R. W. 1962, *Numerical Methods for Scientists and Engineers* (New York: McGraw-Hill).

Lippert, W. 1955, *Optik, 12,* 173–180.

Möllenstedt, G. and Rang, O. 1951, *Z. angew. Phys., 3,* 187–189.

Schiekel, M. 1952, *Optik, 9,* 145–153.

Wilska, A. P. and den Boer, J. A. 1964, *Comm. LPL, 3,* no. 46.

Zworykin, V. K., *et al.* 1954, *Electron Optics and the Electron Microscope* (New York: Wiley).